1

Numerical Dispersion of a Vector Finite Element Method on Skewed Hexahedral Grids

Daniel A. White
Lawrence Livermore National Laboratory

June 14, 1999

Abstract

The numerical dispersion relation is an important measure of the discretization error inherent in grid-based numerical methods for solving Maxwell's equations. In this paper we calculate the numerical dispersion of a vector finite element method for the case of a distorted three-dimensional hexahedral grid. The main result is that the numerical dispersion relation remains second-order accurate as the grid is distorted, although the dispersion becomes quite anisotropic.

1 Introduction

The classic nodal finite element method has been shown to be an accurate and robust method for solving electrostatic problems on three-dimensional unstructured grids. However the use of nodal finite elements for fully electromagnetic problems has been problematic for several reasons. First, the standard Lagrange nodal finite element does not allow jump discontinuities of fields across material interfaces. Second, the use of nodal finite elements can lead to spurious, non-physical solutions. For these reasons, vector finite element methods which employ the recently developed class of elements known as edge, Nedelec, or $H(curl)$ elements [1, 2, 3, 4, 5] have become quite popular. This paper is concerned with the numerical dispersion of a vector finite element method employing linear hexahedral edge elements. The analysis is applicable to either frequency domain or time domain formulations.

The numerical dispersion relation is useful for determining if a method is consistent, and it gives the order (rate of convergence) of the method. Engineers can use the numerical dispersion relation to determine the grid resolution required to achieve a certain accuracy. It is well known that the classic FDTD method has a second-order accurate numerical dispersion

* D. A. White, e-mail dwhite@llnl.gov, fax 510-423-2993.

This work was supported in part by the U.S. Department of Energy under Grant No. W-7405-Eng-48.

relation [6]. The numerical dispersion relation has been derived for vector finite element methods on two-dimensional square [7] and triangular [8, 9, 10] grids. In this paper a procedure for obtaining the numerical dispersion relation for three-dimensional distorted hexahedral grids is described. The main result is that the numerical dispersion relation remains second-order accurate for distorted grids, although the numerical dispersion can become quite anisotropic.

2 Galerkin Formulation

We are concerned with the computer simulation of time dependent electromagnetic fields in a generic volume Ω. There is no free charge in the volume. An appropriate PDE is the vector wave equation for the electric field $\vec{E}$

$$\epsilon \frac{\partial^2}{\partial t^2}\vec{E} = -\nabla \times \mu^{-1}\nabla \times \vec{E} - \frac{\partial}{\partial t}\vec{J} \text{ in } \Omega. \tag{1}$$

For simplicity it is assumed that the dielectric permittivity ϵ and the magnetic permeability μ are constant scalars. The electric field on the boundary Γ is specified by

$$\hat{n} \times \vec{E} = \vec{E}_{bc} \text{ on } \Gamma, \tag{2}$$

and the two initial conditions

$$\vec{E}(t=0) = \vec{E}_{ic} \text{ in } \Omega, \tag{3}$$

$$\frac{\partial}{\partial t}\vec{E}(t=0) = \frac{\partial}{\partial t}\vec{E}_{ic} \text{ in } \Omega, \tag{4}$$

complete the description of the PDE. Typically the initial conditions are zero and the problem is driven by either the time dependent current source $\vec{J}$ or the time dependent boundary condition $\vec{E}_{bc}$.

The variational form of (1) is: find $\vec{E} \in H(curl)$ that satisfies

$$\frac{\partial^2}{\partial t^2}\left(\epsilon\vec{E}, \vec{E}^\star\right) = \left(\mu^{-1}\nabla \times \vec{E}, \nabla \times \vec{E}^\star\right) - \frac{\partial}{\partial t}\left(\vec{J}, \vec{E}^\star\right) \tag{5}$$

for all $\vec{E}^\star \in H_0(curl)$, where

$$(\vec{u}, \vec{v}) = \int_\Omega \vec{v} \cdot \vec{u} d\Omega, \tag{6}$$

and

$$H_0(curl) = \left\{\vec{v} : \vec{v} \in H(curl), \hat{n} \times \vec{v} = 0\right\}. \tag{7}$$

In the finite element solution of (5) the space $H(curl)$ is approximated by a finite dimension subspace $W^h \subset H(curl)$ defined on a mesh, yielding a system of ODE's

$$A\frac{\partial^2}{\partial t^2}\tilde{e} = C\tilde{e} + \tilde{s}. \tag{8}$$

The variable $\tilde{e}$ is the array of degrees of freedom (DOF) and the variable $\tilde{s}$ is the array of source terms, which includes contributions from both the independent current source $\vec{J}$ and the boundary condition $\vec{E}_{bc}$. The

matrix A is a symmetric positive definite matrix, with units of capacitance, which resembles the mass matrix of continuum mechanics. The matrices A and C are given by

$$A_{ij} = \left(\epsilon \vec{W}_i, \vec{W}_j\right), \tag{9}$$

$$C_{ij} = \left(\mu^{-1} \nabla \times \vec{W}_i, \nabla \times \vec{W}_j\right), \tag{10}$$

where $\vec{W}_i$ is the basis function associated with edge i. The system of ODE's (8) is integrated using the leapfrog method, which requires the linear system to be solved at every time step. An efficient method for solving this system is described in [11], and the stability of the method is discussed in [12].

For every hexahedral cell there are 12 edge basis functions. It is convenient to define the basis functions on a unit cube and then transform the functions appropriately. First, define the polynomial space $Q_{l,m,n}$ in three variables x, y, and z the maximum degree of which are respectively, l in x, m in y, and n in z. The polynomial space P used for the linear edge element is

$$P = \{\vec{u} : u_x \in Q_{0,1,1}; u_y \in Q_{1,0,1}; u_z \in Q_{1,1,0}\}. \tag{11}$$

The basis functions $\vec{W}_i$ are then defined by the equation

$$\int \vec{W}_i \cdot \vec{t}_j ds = \delta_{ij}, \tag{12}$$

where $\vec{t}_j$ is the unit tangent along edge j. If the cubical cell is distorted according to the isoparametric transformation

$$\tilde{x} = B\vec{x} + \vec{b}, \tag{13}$$

the vector basis functions must be transformed covariantly,

$$\vec{W} = B^{-1}\tilde{W}. \tag{14}$$

3 Numerical Dispersion

In an infinite, homogeneous, source-free region the solution of (1) is a plane wave of the form

$$\vec{E} = \vec{E}_0 e^{I\left(\vec{k}\cdot\vec{x} - \omega t\right)}, \tag{15}$$

where ω is the radian frequency, $\vec{k}$ is the wave vector, and $\vec{E}_0$ is a constant vector perpendicular to $\vec{k}$ that determines the polarization of the wave. The above equation is the Fourier representation of a plane wave with $I = sqrt{-}1$. The plane wave is a solution to (1) only if the dispersion relation

$$\omega^2 = c^2 k^2, \tag{16}$$

is satisfied, where $c = 1/\sqrt{\mu\epsilon}$ is the speed of light and k is the wave number. The phase velocity is given by

$$\nu = \frac{\omega}{k} \tag{17}$$

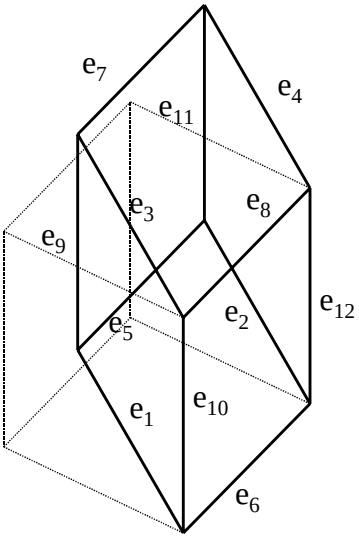

Figure 1: Definition of edge numbering scheme

which is equal to the speed of light c.

The vector finite element method, like other grid-based schemes for solving Maxwell's equations, exhibits numerical dispersion and numerical anisotropy due to the finite grid and the finite time sampling. A numerical wave propagating on a grid will not satisfy (16) in general. The numerical dispersion relation is derived by assuming a discrete plane wave solution, and solving for ω in terms of k.

For this analysis a cubical cell is distorted such that edges e_1-e_4 are parallel, edges e_5-e_8 are parallel, and edges e_9-e_{12} are parallel. This is illustrated in Fig. 1. Since the solution is a plane wave of arbitrary polarization, $\vec{E}_0$ has three components, denoted by X, Y, and Z. The electric field DOF on edges e_1-e_4 are related by

$$\begin{aligned} e_1 &= X \\ e_2 &= Xe^{I\left(\vec{k}\cdot\Delta_2-\omega\Delta t\right)} \\ e_3 &= Xe^{I\left(\vec{k}\cdot\Delta_3-\omega\Delta t\right)} \\ e_4 &= Xe^{I\left(\vec{k}\cdot\Delta_4-\omega\Delta t\right)} \end{aligned} \tag{18}$$

where Δ_i is the distance from edge e_1 to edge e_i. Likewise, for edges e_5-e_8 we have

$$\begin{aligned} e_5 &= Y \\ e_6 &= Ye^{I\left(\vec{k}\cdot\Delta_6-\omega\Delta t\right)} \\ e_7 &= Ye^{I\left(\vec{k}\cdot\Delta_7-\omega\Delta t\right)} \\ e_8 &= Ye^{I\left(\vec{k}\cdot\Delta_8-\omega\Delta t\right)} \end{aligned} \tag{19}$$

where Δ_i is the distance from edge e_5 to edge e_i. Finally, the electric field DOF on edges e_9-e_{12} are related by

$$\begin{aligned} e_9 &= Z \\ e_{10} &= Ze^{I\left(\vec{k}\cdot\Delta_{10}-\omega\Delta t\right)} \\ e_{11} &= Ze^{I\left(\vec{k}\cdot\Delta_{11}-\omega\Delta t\right)} \\ e_{12} &= Ze^{I\left(\vec{k}\cdot\Delta_{12}-\omega\Delta t\right)} \end{aligned} \tag{20}$$

where Δ_i is the distance from edge e_9 to edge e_i.

For time domain simulation the time derivative will be approximated by the second-order central difference formula

$$\left(\frac{\partial^2 e}{\partial t^2}\right)^n \approx \frac{e^{n+1}-2e^n+e^{n-1}}{\Delta t^2}, \tag{21}$$

where n denotes the the discrete time index. Since we are assuming a time harmonic field, the time derivative can be expressed as

$$\frac{\Psi e}{\Delta t^2}, \tag{22}$$

where

$$\Psi = 2\left(\cos\left(\omega\Delta t - 1\right)\right). \tag{23}$$

Combining (8)- (10) and (18)-(20) yields a homogeneous system of equations

$$\left(\Psi F + \eta G\right) \left| \begin{array}{c} X \\ Y \\ Z \end{array} \right| = 0 \tag{24}$$

for X, Y, and Z. In (24) $\eta = c^2\frac{\Delta t^2}{\Delta h^2}$ is a given constant, where the Δh^2 term is pulled out of the integrals in (9) and (10). The 3 by 3 matrices F and G are functions of the phase factors $e^{I\left(\vec{k}\cdot\Delta-\omega\Delta t\right)}$ and the matrices A and C, respectively. The matrices F and G are complicated and will not be shown here. The reader is referred to [12] for a complete description of these matrices.

The numerical dispersion relation is given by

$$det\left(\Psi F + \eta G\right) = 0. \tag{25}$$

This is a complicated non-linear relationship between $\vec{k}$ and ω. There are three roots: one is zero which does not represent anything physical; the other two are equal and correspond to the two distinct polarizations. For a given grid, the roots of (25) can be computed using a symbolic math package such as Mathematica. Given these roots, it is possible to pick a value of $\vec{k}$ and solve for ω. The numerical phase velocity is then given by (17).

Consider a unit cube with a skew distortion by an amount θ in the x direction and by the same amount θ in the z direction as shown in Fig. 1. Let

$$\vec{k} = k\left(\hat{x}\cos(\alpha)\sin(\beta) + \hat{y}\sin(\alpha)\sin(\beta) + \hat{z}\cos(\beta)\right) \tag{26}$$

be the wave vector with spherical angles α and β. The numerical phase velocity is then a function of θ, α, β, and k. In the computational experiments below $c = 1$, $\Delta h = 1$, and $\Delta t = 1/3$. Figures 2 through 5 show surfaces of phase velocity error for sheer angles of $\theta = 0°$, $\theta = 15°$, $\theta = 30°$, and $\theta = 45°$, respectively. Each figure shows the velocity error for $k = 2\pi/5$, with the velocity error defined as $\nu - c$. The figures clearly show that the numerical phase velocity becomes quite anisotropic for large skew angles.

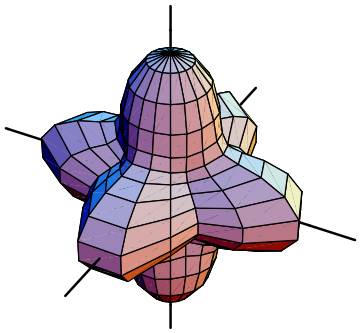

Figure 2: Phase velocity error for $\theta = 0°$. The length of the axis is 0.15 m/s

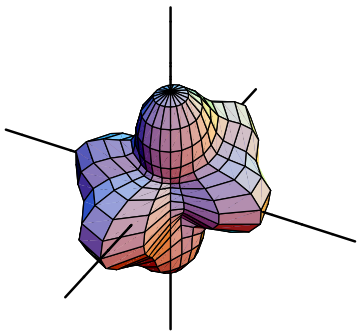

Figure 3: Phase velocity error for $\theta = 15°$. The length of the axis is 0.25 m/s

The velocity error in Figures 2 through 5 is fairly large due to the $\lambda/5$ grid spacing. The minimum velocity, maximum velocity, and anisotropy ration are tabulated below as a function of k for each of the four grid distortions. The error is reduced significantly as k decreases, as expected. It is possible to determine the rate of convergence of the numerical dispersion relation by applying a least-square fit to the data in Tables 1 through

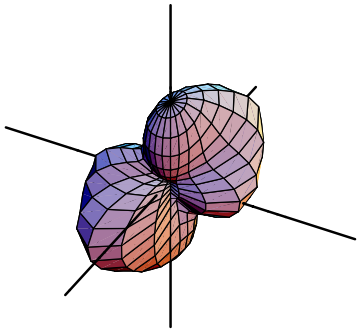

Figure 4: Phase velocity error for $\theta = 30°$. The length of the axis is 0.35 m/s

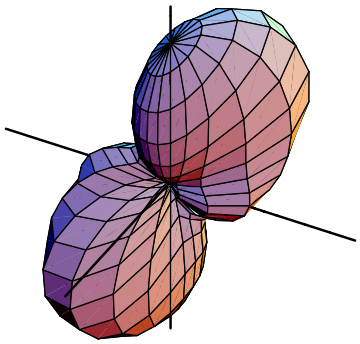

Figure 5: Phase velocity error for $\theta = 45°$. The length of the axis is 0.35 m/s

4. The logarithm of the error versus the logarithm of k is shown in Fig 6 for each of the four grids, along with a least-square fit. The least-square fit is applied to the maximum velocity error. For each grid the slope of the linear fit is approximately 2 (from 2.02 to 2.09), indicating second-order convergence.

By performing a Taylor series expansion of the roots of (25), with respect to $\omega\Delta t$ and $k\Delta h$, it can be shown that the numerical dispersion relation has the form

$$\frac{\omega^2}{k^2} = c^2 \frac{1 + O\left((k\Delta h)^2\right)}{1 - 1/12\,(\omega\Delta t)^2 + O\left((\omega\Delta t)^4\right)}. \tag{27}$$

The denominator represents the isotropic part of the dispersion, and the numerator represents the anisotropic part. The numerical dispersion for a frequency domain method is obtained by simply setting $\Delta t = 0$. Thus the shape of the numerical dispersion surfaces shown in Figures 2 through

Table 1: Phase velocity and anisotropy ratio for $\theta = 0$ grid

k	max ν	min ν	ratio
2 π / 5	1.07538	1.03002	1.04404
2 π / 10	1.01845	1.00736	1.01101
2 π / 15	1.00816	1.00326	1.00488
2 π / 20	1.00458	1.00183	1.00274

5, and the anisotropy ratio tabulated in Tables 1 through 4, is the same for time or frequency domain implementations.

Table 2: Phase velocity and anisotropy ratio for $\theta = 15$ grid

k	max ν	min ν	ratio
2 π / 5	1.08797	1.01709	1.06969
2 π / 10	1.02113	1.00423	1.01682
2 π / 15	1.00931	1.00188	1.00742
2 π / 20	1.00522	1.00106	1.00416

Table 3: Phase velocity and anisotropy ratio for $\theta = 30$ grid

k	max ν	min ν	ratio
2 π / 5	1.14536	1.00913	1.135
2 π / 10	1.03401	1.00227	1.0316
2 π / 15	1.01493	1.00101	1.0139
2 π / 20	1.00836	1.00057	1.00779

Table 4: Phase velocity and anisotropy ratio for $\theta = 45$ grid

k	max ν	min ν	ratio
2 π / 5	1.35058	1.00333	1.34609
2 π / 10	1.08656	1.00083	1.08566
2 π / 15	1.03845	1.00037	1.03807
2 π / 20	1.02163	1.00021	1.02142

4 Conclusion

A procedure for determining the numerical dispersion of a vector finite element method on three-dimensional distorted hexahedral grids was presented. For the class of grid distortions analyzed, the numerical dispersion relation remains second-order accurate as the grid is distorted. However,

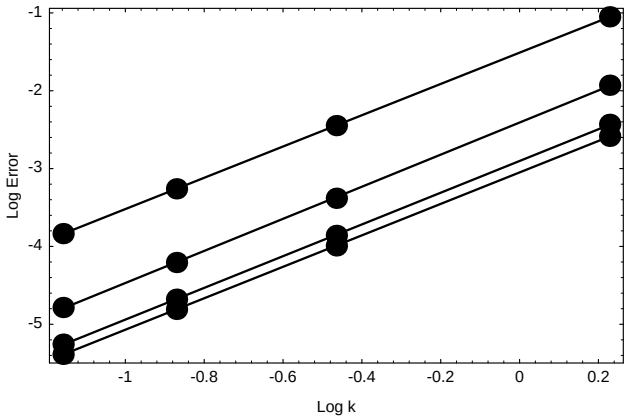

Figure 6: Least-square fit of velocity error indicating second-order convergence. The larger error corresponds to larger grid sheer angle.

the numerical dispersion relation becomes quite anisotropic as the grid is distorted. For example, the maximum phase error for a 30° skew distortion grid is twice that of a uniform Cartesion grid.

References

[1] Nedelec, J. C., "Mixed finite elements in R3," *Numer. Math.*, 35, pp. 315–341, 1980.

[2] Bossavit A., "Whitney forms: a class of finite elements for three-dimensional computations in electromagnetism," *IEE Proceedings*, v. 135, pt. A, n. 8, pp. 493–500, 1988.

[3] Bossavit A. and Mayergoyz I., "Edge elements for scattering problems," *IEEE Trans. Mag.*, v. 25, n. 4, pp. 2816–2821, 1989.

[4] Cendes Z. J., "Vector finite elements for electromagnetic field problems," *IEEE Trans. Mag.*, v. 27, n. 5, pp. 3958–3966, 1991.

[5] Lee J. F., Sun D. K., and Cendes Z. J., "Tangential vector finite elements for electromagnetic field computation," *IEEE Trans. Mag.*, v. 27, n. 5, pp. 4032–4035, 1991.

[6] Kunz K. and Luebbers R., *The Finite Difference Time Domain Method for Electromagnetics*, CRC Press, Boca Raton, Florida, 1993.

[7] Warren S. and Scott W., "An investigation of numerical dispersion in the vector finite element method using quadrilateral elements," *IEEE Trans. Ant. Prop.*, v. 42, n. 11, pp. 1502-1508,1994.

[8] Monk P. and Parrot A., "An dispersion analysis of finite element methods for Maxwell' equations," *SIAM J. Sci. Comput.*, v. 15, n. 4, pp. 916-937,1994.

[9] Warren S. and Scott W. "Numrical dispersion in the finite element method using triangular edge elements," *Micro. Opt. Tech. Lett*, v. 9, n. 6, pp. 315-319,1995.

[10] White D. and Rodrigue G., "Improved vector FEM solutions of Maxwell's equations using grid preconditioning," *Int. J. Num. Meth. Eng.*, v. 40, n. 20, pp. 3815–3837, 1997.

[11] White D., "Solution of Capacitance Systems using Incomplete Cholesky Fixed Point Iteration," submitted to *Comm. Num. Meth. Eng.*

[12] White D., "Discrete time vector finite element methods for solving Maxwell's equations on 3D unstructured grids," Ph.D. Dissertation, University of California at Davis, Sept. 1997.